Progress In Electromagnetics Research C, Vol. 126, 1–11, 2022

Study on Electromagnetic Vibration Performance of Hybrid Excitation Double Stator BSRM for Flywheel Battery under Eccentricity

Qianwen Xiang, Zhende Peng*, and Yu Ou

Abstract—In this paper, the electromagnetic vibration characteristics of hybrid excitation double-stator Bearingless Switched Reluctance Motor (HEDSBSRM) used in flywheel battery are analyzed when the rotor is eccentric. Firstly, the influence of rotor eccentricity on motor vibration is theoretically analyzed. Then the finite element method is adopted to study the radial electromagnetic force of the motor in the two-dimensional air-gap region. In addition, the three-dimensional equivalent vibration model of the motor outer stator is established, and the mode shapes and natural frequencies of the motor stator are obtained by the modal analysis. The vibration characteristics of the outer stator under eccentric motion are analyzed by the coupling calculation of electromagnetic field and mechanical field. Finally, the modal combination principle is used to analyze the vibration characteristics of the motor running at multiple speeds under eccentric condition. The results show that the vibration of HEDSBSRM is closely related to eccentricity, which affects the motor performance and lays the foundation for the optimization design of HEDSBSRM application in flywheel battery.

1. INTRODUCTION

With the increasing aggravation of energy crisis, the proportion of flywheel battery is increasing in the field of new energy. As the core component of flywheel battery, motor makes flywheel battery more critical to motor performance. Hybrid excitation double stator bearingless switched reluctance motor (HEDSBSRM) has advantages of no mechanical bearing and small loss and solves the problem of the coupling between torque and suspension system of traditional BSRM. BSRM achieves high output power and high speed operation, which meets the requirements of flywheel battery for motor performance. Therefore, BSRM has good prospects in flywheel battery application [1–3].

HEDSBSRM produces electromagnetic vibration by electromagnetic force when operating in practice, which leads to potential risk in the application of flywheel battery. There are less research on electromagnetic vibration of HEDSBSRM at present. Due to the large rigidity of rotor and closed inner stator of HEDSBSRM, the inner stator directional excitation generates the suspension force, and outer stator three-phase alternating excitation generates torque. Thus, the outer stator is the main source of vibration. The phase current of outer stator is discontinuous. During the commutation period, the radial force of outer stator air gap will change dramatically. In the meanwhile, the outer stator is deformed by radial force and generating vibration. The generating electromagnetic vibration is more obvious when the radial force frequency is close to the natural frequency of the outer stator [4–6].

Motor rotor eccentricity is unavoidable due to the error in processing and assembly and the rotor affected by centrifugal force during operation. Eccentricity contributes to uneven stator and rotor air gap and unbalanced magnetic pull, which affects magnetic field variation and leads to new frequency

Received 6 October 2022, Accepted 4 November 2022, Scheduled 16 November 2022
* Corresponding author: Zhende Peng (1511471940@qq.com).
The authors are with the School of Electrical and Information Engineering, Jiangsu University, China.

components emerging in the radial force waves eventually. The mathematical model of BSRM radial force is obtained by the analysis of the eccentric air gap magnetic density in [7, 8]. It is acquired that the radial force varies nonlinearly with the rotor position angle of the excitation current. According to eccentric magnetic field distribution, [9] concludes that radial force is an increasing function of eccentric displacement. Reference [10] indicates that eccentricity would increase new vibrational forms of BSRM.

In order to predict the vibration of HEDSBSRM accurately, guide the low noise design of motor to more fit the performance requirements of flywheel battery, and improve energy conversion efficiency, the influence of the rotor eccentricity on electromagnetic vibration is non-negligible. At present, there are few articles on BSRM eccentric vibration, especially the effect of eccentricity on double stator BSRM. This paper first introduces the operating mechanism of HEDSBSRM and characteristics of the radial force of outer stator during the rotor eccentricity. Then finite element method is adopted to analyze the harmonic component of the outer stator radial force under different eccentricities. Additionally, the vibration shapes and natural frequencies of the outer stator are obtained by comparing and combining modal analysis. Establish the electromagnetic-vibration simulation model and analyze the influence of eccentricity on motor vibration response. Finally, motor vibration response under different eccentric states at multiple speeds is analyzed based on harmonic response.

2. OPERATION MECHANISM

HEDSBSRM is composed of a 24 pole outer stator, a 16 pole rotor, an 8 pole inner stator, and 4 permanent magnets. Fig. 1 is motor topology diagram. The outer stator is divided into A, B, and C phases which together with rotor provide rotor rotation force according to the torque minimum principle. The inner stator winding and permanent magnet work together to provide the suspension force. Taking x-direction as an example, when the rotor shifts in positive x-direction, the magnetic flux generated by inner stator winding and the magnetic flux generated by permanent magnet overlay in positive x-direction, and the magnetic field increases, generating the suspension force in negative x-direction to make the rotor in a balanced position. Torque and suspension system achieve decoupling, with good speed and suspension performance, which are quite suitable for the application in flywheel batteries.

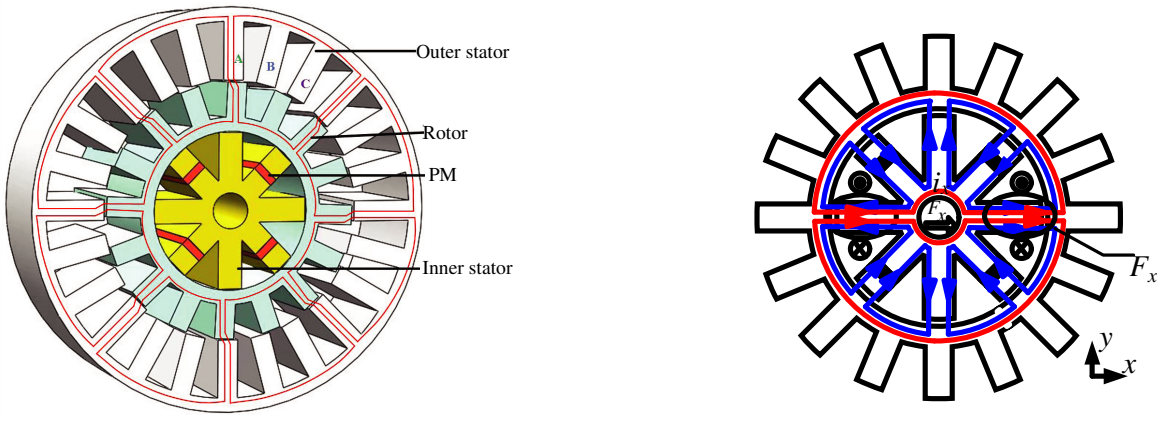

(a) Torque (b) Suspension force F_x

Figure 1. Topology of HEDSBSRM.

3. ECCENTRIC RADIAL ELECTROMAGNETIC FORCE MODELING

3.1. Radial Electromagnetic Force Analysis

According to the integration of Maxwell stress tensor on inner surface of outer stator core or outer surface of rotor, the radial electromagnetic force wave is [11]:

$$p_r(\theta,t) = \frac{b_r^2(\theta,t)}{2\mu_0} \tag{1}$$

In the formula, μ_0 is the permeability of vacuum, whose value is $4\pi \times 10{-}7\,\mathrm{H/m}$, and $b_r(\theta,t)$ is radial air gap magnetic density which is the function of time and spatial location. Without considering the magnetic saturation, it can be expressed as:

$$b(\theta,t) = f(\theta,t)\Lambda(\theta,t) \tag{2}$$

In the formula, $f(\theta,t)$ is air-gap magnetic potential; $\Lambda(\theta,t)$ is the air-gap permeance. Ignoring the current harmonics, the air gap magnetic potential can be expressed as:

$$f(\theta,t) = \sum_{k=1}^{\infty} f_k \cos(p\omega t \pm kp\theta + \phi) \tag{3}$$

k is the number of magnetic field harmonics, and when the influence of saturation and stator and rotor slots and the eccentricity is disregarded, the motor air gap magnetic permeance is:

$$\Lambda_0(\theta,t) = \sum_{k=0}^{\infty} \Lambda_k \cos(kZ\theta) \tag{4}$$

According to (1) (2) (3) (4), the radial electromagnetic force can be expressed as a series of force waves with different frequencies and different distributions, as shown below:

$$p_r(\theta,t) = \sum_{n} p_n \cos(\omega_n t - n\theta + \phi_n) \tag{5}$$

Here $p_r(\theta,t)$ is a radial force wave and is the force per unit area. The unit is $\mathrm{N/M^2}$, and n represents the force wave of order time. ω represents the rotor rotation angular velocity. p_n represents the n-degree force wave amplitude.

3.2. Air-Gap Permeance during Rotor Eccentricity

During the operation process, the rotor of HEDSBSRM will appear in three eccentric states: static eccentric, dynamic eccentric, and hybrid eccentric [12, 13]. Taking static and dynamic eccentricity rotor as an example, the coordinate system is established with the stator center as the origin. As shown in Fig. 2, O is the stator center, O' the rotor center during the rotor eccentricity, R_s the stator inner diameter, and R_r the rotor outer diameter. The stator and rotor air gap during eccentricity can be described as:

$$\delta(\theta) = R_S - R_r + \varepsilon \cos\left(\theta - \alpha - \gamma\frac{\omega}{p}t\right) \tag{6}$$

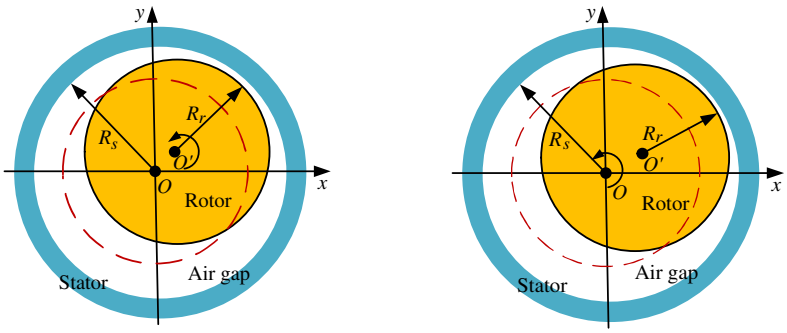

(a) Static Eccentricit (b) Dynamic Eccentricity

Figure 2. Schematic diagram of motor eccentricity.

where ε is the eccentricity, and θ is the relative position angle of the stator and rotor. γ is different eccentric type, and $\gamma = 1$ indicates a static eccentricity while $\gamma = 2$ indicates the dynamic eccentricity. Eccentricity ε is defined as:

$$\varepsilon = \frac{r}{\delta} \tag{7}$$

r is the distance from the stator center to the rotor center. δ is the air gap length under normal conditions. At this time, the motor air-gap permeance during eccentricity is:

$$\Lambda(\theta, t) = \sum_{k=0}^{\infty} \Lambda_k \cos(kZ\theta)(1 - \varepsilon \cos\gamma\theta) = \Lambda_0(\theta, t) - \varepsilon \cos\gamma\theta \sum_{k=0}^{\infty} \Lambda_k \cos(kZ\theta) \tag{8}$$

New components apparently appear in the eccentric air-gap permeance. The second part is defined as the eccentric magnetic permeability part. Combining with Formulas (1) and (2), the eccentric radial electromagnetic force of the outer stator will produce a new order and frequency. If the new radial force frequency is close to the natural frequency of the outer stator, the vibration response of the motor is more obvious.

4. FINITE ELEMENT ANALYSIS OF ECCENTRIC RADIAL ELECTROMAGNETIC FORCE OF OUTER STATOR

4.1. Finite Element Analysis of the Outer Stator Radial Electromagnetic Force

The relation between outer stator vibration amplitude A_m and electromagnetic force wave of HEDSBSRM:

$$A_m \propto \frac{F_m}{(v^2 - 1)^2} \left[\frac{1}{1 - (f/f_c)^2} \right] \tag{9}$$

where F_m is the radial electromagnetic force amplitude of the outer stator, v the spatial force wave order, f the force wave frequency, and f_c the outer stator intrinsic frequency. It is observed that A_m is directly proportional to F_m and is approximately inversely proportional to the 4th power of v. Therefore, the lower the order is, the stronger the vibration is. When f and f_c are close, the motor also produces a relatively large vibration noise. Thus the design should be considered to avoid making the motor produce a resonant frequency. For the 24/16/8 HEDSBSRM, the time order u and space order v of the outer stator air gap radial force harmonic component can be expressed by (10) [14, 15]:

$$\begin{cases} u = (m \times Z_r) \times j + Z_r \times k = 48 \times j + 16 \times k \\ v = \dfrac{Z_s}{Z_r} \times k = 8 \times k \end{cases} \tag{10}$$

where m is the motor phase number, Z_r the rotor pole number, and Z_s the stator pole number. j and k are arbitrary integers. Therefore, the low-order space order of the motor is 0, 8, and 16, and the time order is 0, 16, 32, and 48.

The radial electromagnetic force density generated by the A-phase winding excitation of the outer stator of HEDSBSRM is fast Fourier decomposition. As shown in Fig. 3, there are radial forces of $v = 0$ and $v = 8$ respectively for the blue and green columns in the figure. And the radial electromagnetic force amplitude value is larger when the base frequency is 0 times, 1 time, and 2 times. The frequency here corresponds to time order 0, 16, and 32, respectively. The results are consistent with the previous theoretical analysis. However, the 0 time base frequency is 0, and it will not cause vibration [16]. Therefore, the influence of 1 time base frequency and 2 time base frequency on motor vibration are focused on. This frequency should be avoided as close to the natural frequency of the motor during motor operation which may cause large vibration.

4.2. Analysis of Eccentricity to Radial Electromagnetic Force

When torque winding of HEDSBSRM is single-phase excited, taking static eccentricity as an example, the radial air gap magnetic density of outer stator along the circular distribution curve is compared

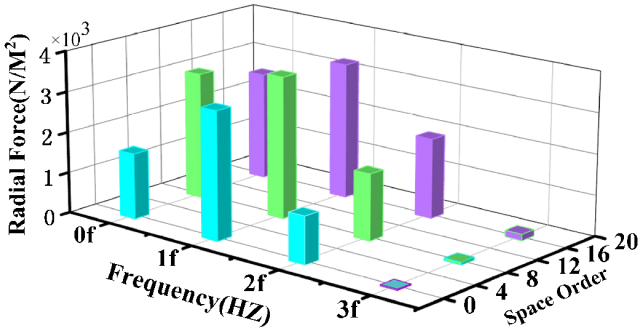

Figure 3. Fourier decomposition of radial electromagnetic force of outer stator.

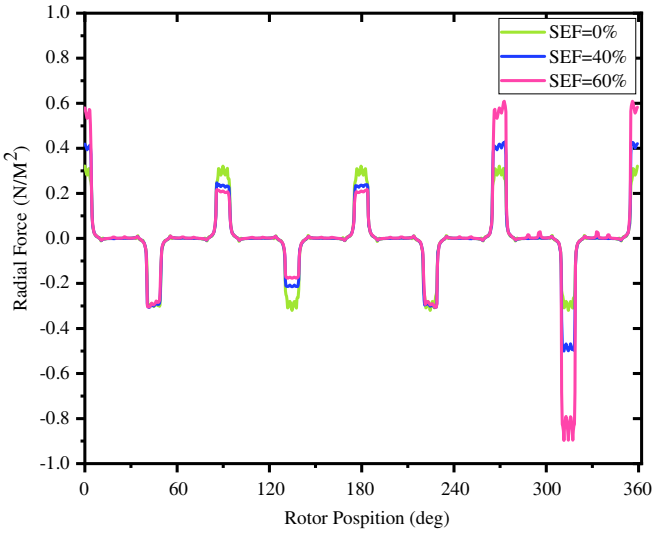

Figure 4. Air gap magnetic density distribution with different eccentricities.

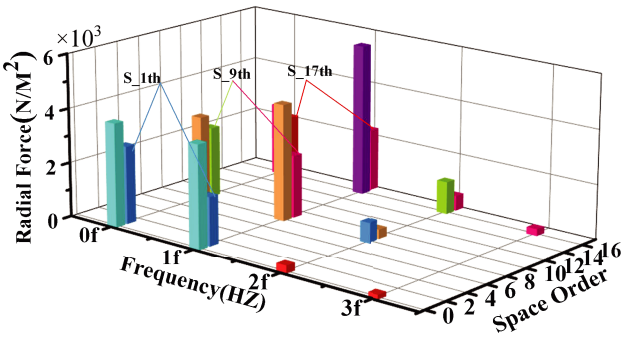

Figure 5. Radial force FFT of outer stator at SEF = 40%.

when static eccentricity (SEF) SEF = 0%, SEF = 40% and SEF = 60%. As shown in Fig. 4, comparative analysis shows that with the increase of eccentricity, the radial magnetic density at the maximum air gap increases significantly. FFT is made to the outer stator radial force when SEF = 40%, as shown in Fig. 5. Compared to no eccentricity in Fig. 3, the radial force increases the number of harmonic components of the lower spatial order of order 1 and order 9. In order to further analyze the influence of eccentricity on motor vibration, the fast Fourier changes of 0 order radial electromagnetic force waves

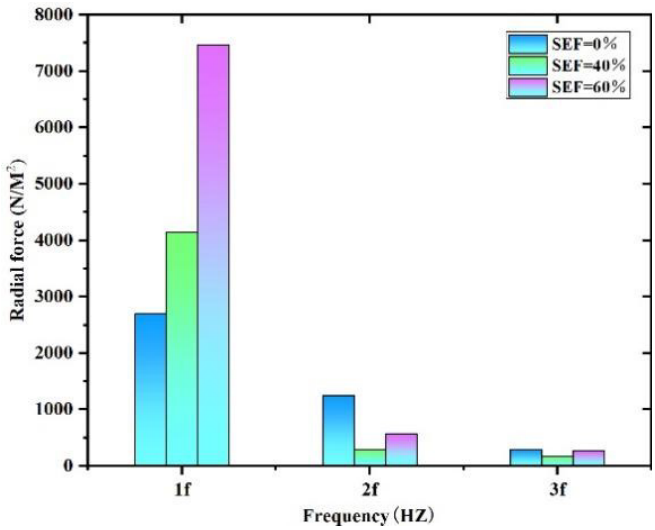

Figure 6. 0 order electromagnetic force spectrum with different eccentricities.

are compared at different rotor eccentricity. As shown in Fig. 6, it is observed that the outer stator radial force amplitude is maximum at 1 time base frequency and increases by 30% with increasing eccentricity. While the eccentricity of the smaller amplitude of 2 and 3 time base frequencies increases, but its amplitude decreases. Based on the above analysis, the rotor eccentricity of HEDSBSRM greatly affects the amplitude and frequency of low-order radial electromagnetic force, and motor electromagnetic vibration is inevitable.

4.3. Analysis of Eccentric Vibration Response of Motor

5. MODAL ANALYSIS AND HARMONIC RESPONSE ANALYSIS

5.1. Modal Analysis of Outer Stator

Modality is the intrinsic vibration property of structure, which includes two layers of meaning of natural vibration type and natural frequency. HEDSBSRM will produce a large vibration phenomenon when the space order of outer stator radial electromagnetic force and outer stator mode order are the same and electromagnetic force frequency are close to the mode natural frequency. The vibration mode of each order and the natural frequency of the corresponding modes can be achieved via modal analysis of the outer stator, avoiding resonance to a certain extent [17–19]. Generally, the low-order mode has a great impact on the motor vibration [20, 21]. The vibration mode and natural frequency of outer stator order $1 \sim 8$ are obtained by finite element method which is compared to experimental method. The experimental method is to tap the outer stator and acquire the signal by sensor and process data to obtain the inherent frequency of object. The experimental data are presented in Table 1. Both errors

Table 1. Outer stator Mode shapes.

Specification	1st Nat. Freq.	2st Nat. Freq.	3nd Nat. Freq.	4th Nat. Freq.	5th Nat. Freq.	6th Nat. Freq.	7th Nat. Freq.
FE analysis	3457 HZ	3688 HZ	3703 HZ	3948 HZ	5383 HZ	5509 HZ	5517 HZ
Experiment	3786 HZ	3710 HZ	3676 HZ	3665 HZ	5346 HZ	5559 HZ	5548 HZ
Differences	8.6%	6.1%	7.3%	4.8%	6.8%	9.1%	5.6%
Mode shapes		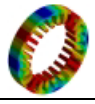	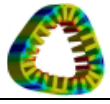	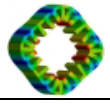	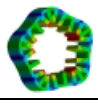	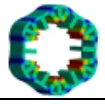	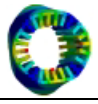

are within 10%, and the finite element model has good validity. According to the above analysis, the eccentricity of the motor will make the radial force of the outer stator increase new frequencies. If these new frequencies are close to the frequency of the outer stator vibration shape obtained from the modal analysis, the motor vibration will be strengthened.

The outer stator radial electromagnetic force is loaded on the stator tooth when HEDSBSRM is performed at 7000 rpm. Fig. 7 is a schematic diagram of radial forces on different eccentric states on an outer stator tooth. When the eccentricity is 60%, the radial force amplitude is the largest, which means that the fluctuation is more obvious when the amplitude of the stator tooth is larger as the degree of eccentricity increases. In addition to the frequency of 0 HZ, the most stressed frequency points of the stator teeth occur in turn around 1866 HZ, 3732 HZ, and 5598 HZ. The three frequencies correspond to 1, 2, and 3 time base frequencies of the radial electromagnetic force, which is basically consistent with the Fourier decomposition results of the electromagnetic force in the upper section.

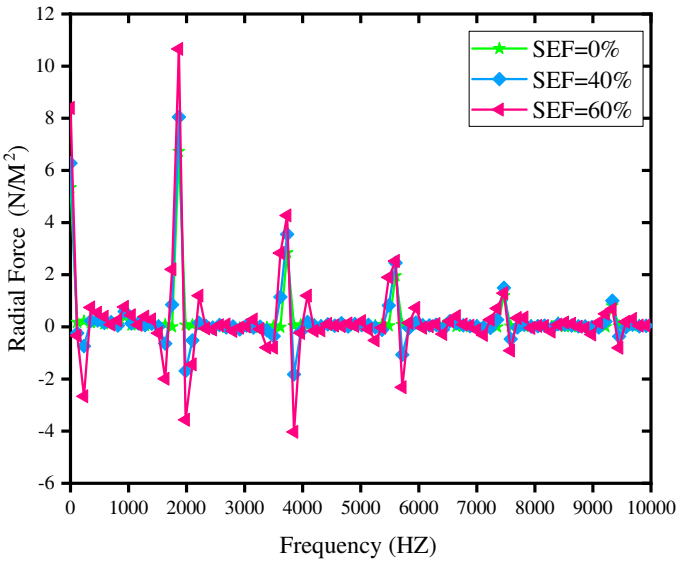

Figure 7. The magnitude of force in different eccentric states on a tooth.

Figure 8(a) is the curve of maximum shape variation of stator teeth varying with frequency in different eccentric states within the $0 \sim 8000$ HZ frequency range. It is observed that the deformation quantity is the most obvious when frequency $f = 3732$ HZ followed by 5598 HZ, and the dependent variable is different under different eccentricities. The deformation quantity decreases a little when SEF = 40% and increases significantly when SEF = 60%. Fig. 8(b) is the acceleration frequency spectrum of different eccentric states when the stator tooth is deformed. It is observed that the vibration acceleration is obvious at frequencies of 3732 HZ and 5598 HZ, respectively. The vibration acceleration amplitude is maximum when SEF = 60%, and frequency is around 3732 HZ. The 3732 HZ here corresponds to the 2 time base frequency of radial electromagnetic force, and 5598 HZ corresponds to 3 time base frequency. As known from the modal analysis, the stator natural frequencies of order 1 to 4 are close to those of 3732 HZ, and the order $5 \sim 8$ natural frequency is close to those of 5598 HZ, which shows that the mode order from 1 to 8 is the source of stator vibration mode. Through the vibration response frequency spectrum, the frequency vibration near 3732 HZ is more obvious with the increase of eccentricity. Fig. 9 is comparison of vibration response difference between different eccentric states under 7000 r/min. It can be seen that with the increase of eccentricity, the vibration is more obvious in different eccentric states at 2 time base frequency and 3 time base frequency, which is the same as the above analysis. In conclusion, the base frequency of the outer stator radial electromagnetic force is the main source of motor vibration, and the mode order $1 \sim 4$ is the main vibration mode of motor vibration. With the increase of eccentricity, the vibration response is more obvious.

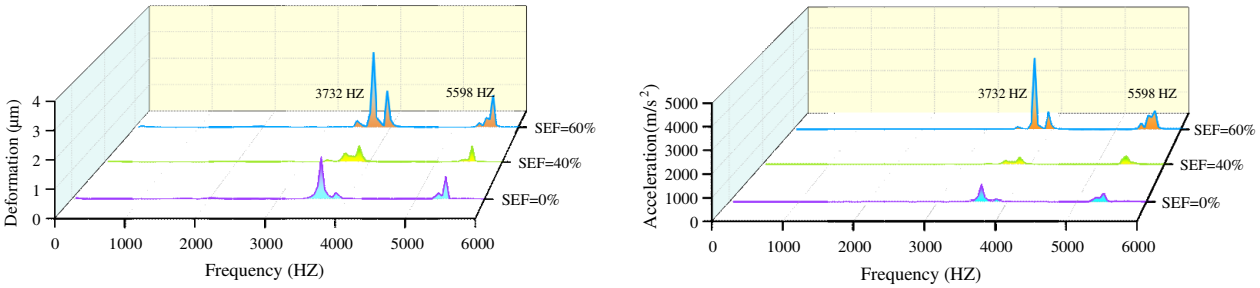

(a) Impact of eccentricity on vibration deformation (b) Impact of eccentricity on vibration acceleration

Figure 8. Impact of eccentricity on vibration response.

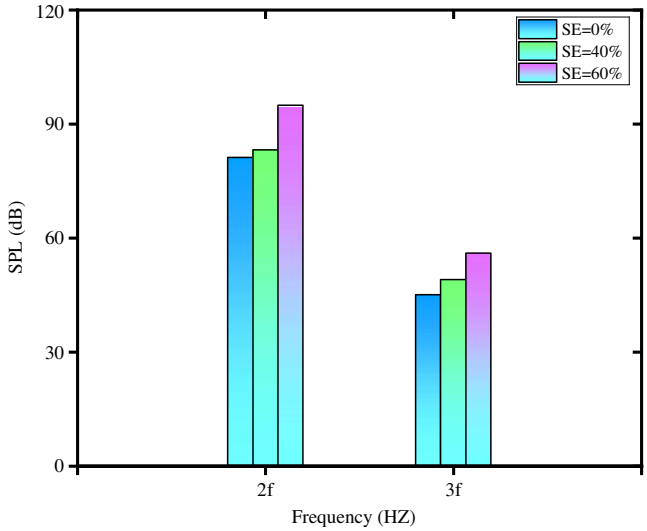

Figure 9. Comparison of vibration response difference.

5.2. Vibration Response Analysis at Multiple RPM

HEDSBSRM needs to be adapted to run at different rotate speeds in the flywheel battery. In order to simulate the actual working conditions and analyze the influence of eccentricity on motor vibration, the vibration response is analyzed at three different eccentricities within the range of 6000 to 1200 r/min, as shown in simulation results of Fig. 10. It can be seen that the vibration at different rotate speeds mainly occurs near the frequencies of 3732 HZ and 5798 HZ, corresponding to the above analysis. SEF = 0% is shown in Fig. 10(a). Near the frequency 3732 HZ, vibrations above 80 dB occur in the velocity ranges of 900 to 1,000 rad/s and 790 to 800 rad/s. Vibrations above 75 dB occur in the velocity range from 660 to 1256 rad/s. Compared to the SEF = 40% in Fig. 10(b), the velocity range of vibration which is greater than 80 dB is reduced to 900 to 980 rad/s and 790 to 800 rad/s, and the frequency range is correspondingly reduced by 10%. The velocity range of vibration which is greater than 75 dB is reduced by 11%, and the frequency range is reduced by 8%. Fig. 10(c) is the vibration frequency spectrum when SEF = 60%. The velocity range is reduced by 12%, and the frequency range is reduced by 9% when producing the same vibration effect compared with no eccentricity. However, the velocity range above 75 dB is from 1021 to 1256 rad/s near 5798 HZ without eccentricity. The velocity range gradually increases when SEF is 40% and 60%, and the velocity range of vibration above 80 dB gradually increases with increasing eccentricity, which means that the vibration effect becomes larger and larger at the same rotate speed. Therefore, the range and amplitude of vibration response gradually decrease with increasing eccentricity at different speeds near 3732 HZ, and the increasing eccentricity causes an enhanced range and amplitude of vibration response around 5798 HZ at different rotate speeds.

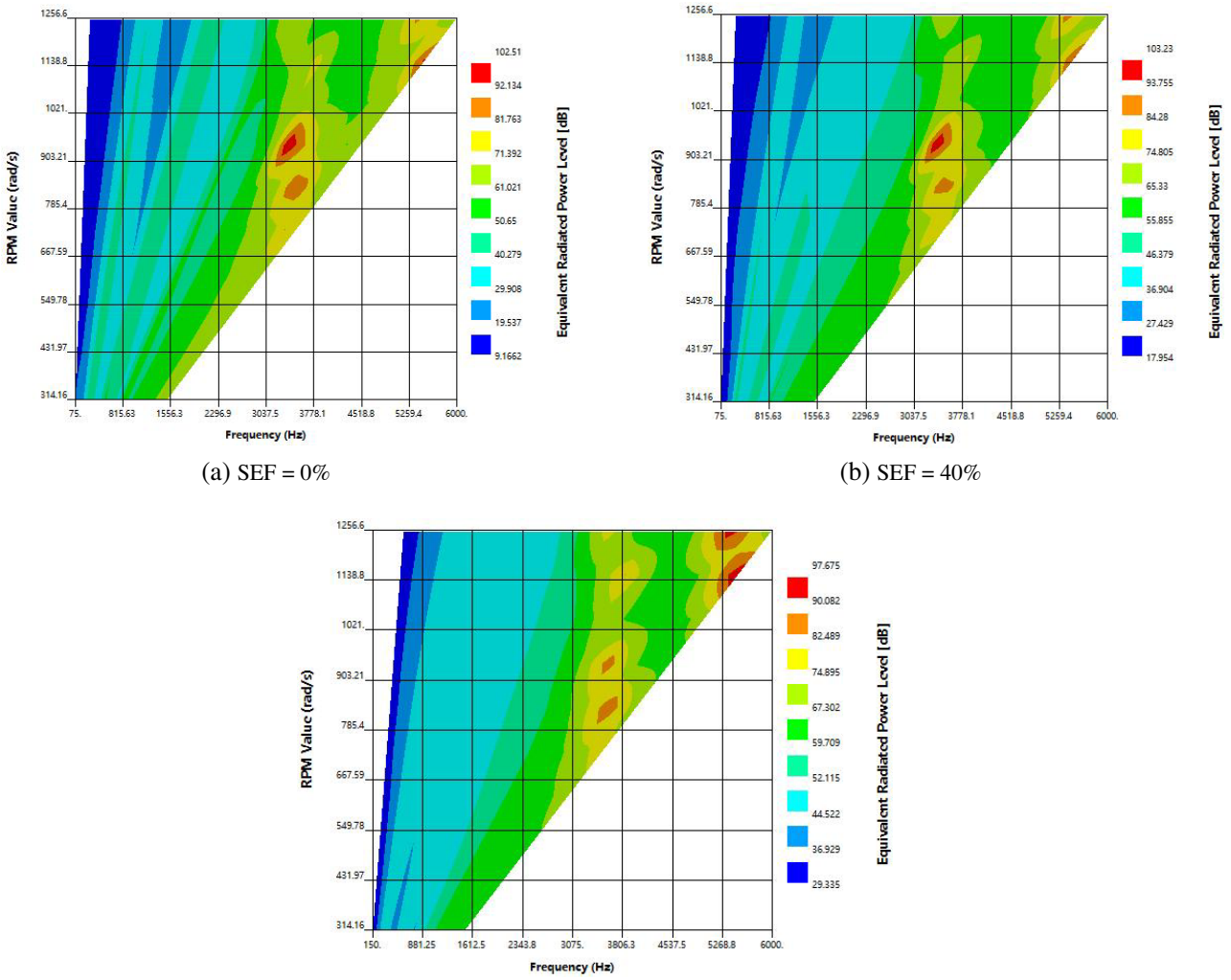

(a) SEF = 0%

(b) SEF = 40%

(c) SEF = 60%

Figure 10. Vibration response analysis at multiple RPM.

It is confirmed by the above analysis that eccentricity affects the electromagnetic vibration performance of HEDSBSRM. The overall vibration response is greater than no eccentricity. Larger vibration levels are observed in a larger velocity range. When designing HEDSBSRM for the flywheel battery, considering the influence of the eccentricity on the vibration performance is essential.

6. CONCLUSION

This paper studies the outer stator radial force influence on the vibration of HEDSBSRM for the flywheel battery taking static eccentricity as an example. The radial forces of the outer stator with different eccentricities were analyzed. The basic mode shapes and natural frequencies of the outer stator were obtained by modal analysis and analyzing the vibration responses of the outer stator with different eccentricities. The results show that the eccentricity increases the new radial force wave component and radial force amplitude, making the vibration more obvious in the same frequency range. Finally, the harmonic response is used to analyze the multiple-speed vibration of the eccentric motor, which shows that the vibration response is different in different eccentric states in the same rotate speed range. This analysis contributes to providing reference for optimizing the motor design in the HEDSBSRM for the flywheel battery, and improving the efficiency of flywheel battery.

REFERENCES

1. Sun, Y., Y. Yuan, Y. Huang, W. Zhang, and L. Liu, "Review of maglev switched reluctance motor and its key technologies," *Transactions of China Electrotechnical Society*, Vol. 30, No. 22, 1–8, 2015.
2. Allirani, S., H. Vidhya, T. Aishwarya, T. Kiruthika, and V. Kowsalya, "Design and performance analysis of switched reluctance motor using ANSYS Maxwell," *2018 2nd International Conference on Trends in Electronics and Informatics (ICOEI)*, 1427–1432, Tirunelveli, 2018.
3. Sun, X., Y. Chen, S. Wang, G. Lei, Z. Yang, and S. Han, "Core losses analysis of a novel 16/10 segmented rotor switched reluctance BSG motor for HEVs using nonlinear lumped parameter equivalent circuit model," *IEEE/ASME Trans. Mech.*, Vol. 23, No. 2, 747–757, Feb. 2018.
4. Isfahani, A. H. and B. Fahimi, "Vibration analysis of a double-stator switched reluctance machine," *2018 IEEE Energy Conversion Congress and Exposition (ECCE)*, 3244–3248, 2018.
5. Gong, C., S. Li, T. Habetler, and P. Zhou, "Acoustic modeling and prediction of ultra-high speed switched reluctance machines based on finite element analysis," *2019 IEEE International Electric Machines & Drives Conference (IEMDC)*, 336–342, 2019.
6. Ru, L., "New stator structure reducing vibration and noise in switched reluctance motor," *2015 18th International Conference on Electrical Machines and Systems (ICEMS)*, 836–839, 2015.
7. Ayari, S., M. Besbes, M. Lecrivain, and M. Gabsi, "Effects of the airgap eccentricity on the SRM vibrations," *IEEE International Electric Machines and Drives Conference. IEMDC'99. Proceedings (Cat. No. 99EX272)*, 138–140, 1999.
8. Chen, L. and W. Hofmann, "Analysis of radial forces based on rotor eccentricity of bearingless switched reluctance motors," *The XIX International Conference on Electrical Machines — ICEM 2010*, 1–6, 2010.
9. Behra, N. and A. K. Pradhan, "Effect of rotor eccentricity in bearingless switched reluctance motor," *2018 Technologies for Smart-City Energy Security and Power (ICSESP)*, 1–6, 2018.
10. Yan, Y., D. Zhiquan, Z. Qianying, and W. Xiaolin, "Stator vibration analysis of bearingless switched reluctance motors," *2010 International Conference on Electrical and Control Engineering*, 1993–1996, 2010.
11. Wang, Y., C. Zhao, and X. Li, "Vibration and noise analysis of flux-modulation double stator electrical-excitation synchronous machine," *IEEE Transactions on Energy Conversion*, Vol. 36, No. 4, 3395–3404, Dec. 2021.
12. Li, J., D. Choi, and Y. Cho, "Analysis of rotor eccentricity in switched reluctance motor with parallel winding using FEM," *IEEE Transactions on Magnetics*, Vol. 45, No. 6, 2851–2854, Jun. 2009.
13. Jia, S., R. Qu, J. Li, Z. Fu, H. Chen, and L. Wu, "Analysis of FSCW SPM servo motor with static, dynamic and mixed eccentricity in aspects of radial force and vibration," *2014 IEEE Energy Conversion Congress and Exposition (ECCE)*, 1745–1753, 2014.
14. Lin, F., S. Zuo, W. Deng, and S. Wu, "Modeling and analysis of acoustic noise in external rotor In-Wheel motor considering Doppler effect," *IEEE Transactions on Industrial Electronics*, Vol. 65, No. 6, 4524–4533, Jun. 2018.
15. Zuo, S., F. Lin, and X. Wu, "Noise analysis, calculation, and reduction of external rotor permanent-magnet synchronous motor," *IEEE Transactions on Industrial Electronics*, Vol. 62, No. 10, 6204–6212, Oct. 2015.
16. Dai, Y., S. Cui, and L. Song, "Finite element modal analysis of vehicle motor," *Proceedings of the CSEE*, Vol. 31, No. 9, 100–104, 2011.
17. Girgis, R. S. and S. P. Vermas, "Method for accurate determination of resonant frequencies and vibration behaviour of stators of electrical machines," *IEE Proceedings. Part B: Electric Power Applications*, Vol. 128, No. 1, 1–11, 1981.
18. Cai, W., P. Pillay, and Z. Tang, "Impact of stator windings and end-bells on resonant frequencies and mode shapes of switched reluctance motors," *IEEE Transactions on Industry Applications*, Vol. 38, No. 4, 1027–1036, 2002.

19. Zhang, X.-B., D. Wang, and Z.-Z. Su, "Stator modal analysis of large split type magnetic bearing motor system," *Journal of Mechanical Engineering*, Vol. 52, No. 8, 1–7, 2016.
20. Wang, H., Z. Wang, Q. Jiang, et al., "Analytical calculation of the natural frequency of switched reluctance motor," *Proceedings of the CSEE*, Vol. 25, No. 12, 133–137, 2005.
21. Wu, J., "Research on stator modes and natural frequencies of switched reluctance motor based on physical model," *Proceedings of the CSEE*, 112–117, Aug. 2004.